Colloid Polym Sci 274:754–762 (1996)

ORIGINAL CONTRIBUTION

T. Skodvin
J. Sjöblom

Dielectric spectroscopy on W/O emulsions under influence of shear forces

Received: 21 September 1995
Accepted: 28 December 1995

Dr. T. Skodvin (✉) · J. Sjöblom
University of Bergen
Department of Chemistry
Allégaten 41
5007 Bergen, Norway

Abstract The dielectric properties of concentrated w/o-emulsions have been investigated, both at rest and during shear. The volume fraction water ranged from 0.50 to 0.95. The time domain dielectric spectroscopy techniques (TDS) was used to record the dielectric spectra, which covered the frequency region from 25 MHz to 2 GHz. In order to simultaneously record rheological and dielectric data a modified viscometer of the coaxial cylinder type was applied.

A close connection between the viscosity and the dielectric properties of w/o emulsions is demonstrated. The very large effects of shear both on the static permittivity and the dielectric relaxation time for the emulsion can partially be ascribed to the degree of flocculation in the system. At high shear rates, at which the emulsions are expected to have a low degree of flocculation, the observed dielectric properties differ from those expected from a theoretical model for spherical emulsion droplets.

Key words W/o emulsions – concentrated – dielectric properties – shear effect on – flocculation

Introduction

Emulsions play an important role both in the industry and in household applications. The use of such systems covers a broad field, ranging from lubrication and cooling of heavy drilling equipment to the more delicate use of creams and ointments in daily beauty care.

However, there may be technological problems connected with the processing of emulsified systems, and in many cases the presence of these systems is undesirable but unavoidable. This calls for reliable methods to both detect the onset of emulsification and to give a quantitative and qualitative description of the emulsion.

Dielectric measurements on heterogeneous colloidal systems have been performed for many years, and the time domain dielectric spectroscopy (TDS) method has been found promising when it comes to investigating w/o-emulsions [1]. In our group we have recently developed equipment for time domain dielectric analysis of these systems in high electric fields in order to study the electrically induced coalescence [2–3]. We have further reported on the dielectric properties of various w/o emulsions, ranging from systems based on crude oils to model margarines [4–7].

It has been demonstrated that the current theoretical models describing the dielectric properties of ideal heterogeneous mixtures [8–11] have severe shortcomings when applied to w/o emulsions. Local variations in the volume fractions disperse phase are not accounted for, thus processes like flocculation and sedimentation must inevitably lead to deviations from these idealized models. We have lately suggested modifications to the existing models by incorporating factors like floc density and shape [5], but there is still ground to be covered before a complete theoretical description can be given.

When flocculated emulsions are subjected to a shearing force, the floc aggregates may disintegrate, rendering an unflocculated system provided the shear rate is sufficiently high. At even higher shear rates the emulsion droplets tend to be deformed, and may even be broken down to smaller units.

In this work we present a new device that may be useful in the investigation of flocculated emulsions. The device is a modified viscometer, in which we have integrated a dielectric sensor. Thus it is possible to perform rheological *and* time domain dielectric measurements simultaneously. In this way we should be able to follow the de-flocculation and other processes by means of two independent experimental techniques. Even though this particular experimental set-up lacks perfection the basic properties and the usefulness of the device are demonstrated.

Theory

Dielectric properties of W/O emulsions

Works by Wagner [12] and Wiener [13], Bruggeman [14] and later Hanai [8–9] have given dielectric models that are applicable on emulsions. The Hanai equation gives the complex permittivity of an emulsion, $\varepsilon^*_{\mathrm{em}}$ as a function of the permittivity of the continuous phase, ε^*_2, the permittivity of the disperse phase, ε^*_1, and the volume fraction ϕ_1, i.e.,

$$\left(\frac{\varepsilon^*_{\mathrm{em}} - \varepsilon^*_1}{\varepsilon^*_2 - \varepsilon^*_1}\right)\left(\frac{\varepsilon^*_2}{\varepsilon^*_{\mathrm{em}}}\right)^{1/3} = 1 - \phi_1 \,. \tag{1}$$

In the derivation of Eq. (1) it is presupposed that the droplets are homogeneously distributed throughout the system, and that the droplets are spherical. In principle it is valid for a complete range of volume fractions, i.e., for $0 \le \phi_1 \le 1$. When subjected to shear forces, or at very high concentrations, one can expect that the emulsion droplets take on a shape different from the spherical. If this is the case, the equations provided for by Boyle [11] or Boned and Peyrelasse [10] may be applied. The Boyle equation, valid for spheroidal inclusions with a parallel alignment, reads

$$\left(\frac{\varepsilon^*_{\mathrm{em}} - \varepsilon^*_1}{\varepsilon^*_2 - \varepsilon^*_1}\right)\left(\frac{\varepsilon^*_2}{\varepsilon^*_{\mathrm{em}}}\right)^{A_i} = 1 - \phi_1 \,, \tag{2}$$

while for a random orientation of dispersed spheroidal particles, Boned and Peyrelasse stated

$$\left(\frac{\varepsilon^*_1 - \varepsilon^*_{\mathrm{em}}}{\varepsilon^*_1 - \varepsilon^*_2}\right)\left(\frac{\varepsilon^*_2}{\varepsilon^*_{\mathrm{em}}}\right)^{3d}\left[\frac{\varepsilon^*_2(1+3A)+\varepsilon^*_1(2-3A)}{\varepsilon^*_{\mathrm{em}}(1+3A)+\varepsilon^*_1(2-3A)}\right]^{3K} = 1 - \phi_1 \,. \tag{3}$$

In Eqs. (2) and (3), A_i and A are depolarization factors (or shape factors) along the axes in the spheroids, and are functions of the axial ratio. d and 3K (Eq. (3)) are functions of A. When A_i and A equals 1/3 (i.e., all three axis are identical) Eqs. (2) and (3) are reduced to the Hanai equation.

By inserting the dielectric parameters for the water phase and the oil phase into Eqs. (1), (2) or (3), one may calculate complete theoretical spectra for w/o emulsions at various volume fractions water. When Eqs. (2) and (3) are used, we can also allow for deviations from a spherical geometry of the dispersed droplets. The theoretical spectra display an extra dispersion in addition to the water dispersion. The relaxation time of this extra dispersion is inversely proportional to the conductivity in and the volume fraction of the water phase. Also deviations from sphericity affect the relaxation time and the permittivity levels. This relaxation is observed experimentally, and is associated with the polarization of the interfaces between the water domains and the oil domain.

Given a random orientation, a dispersion of spheroidal droplets will always show higher permittivities than a dispersion of spherical droplets (given equal volume fractions disperse phase). Also in the case where prolate (elongated) droplets are oriented parallel to an external electric field, the permittivity will be higher than for spherical droplets. Oblate droplets, on the other hand, give rise to lower permittivities than spheres.

Effect of flocculation on the dielectric properties of W/O emulsions

It has long been recognized that agglomeration or flocculation of the dispersed particles in a heterogeneous mixture will alter the dielectric properties of the system [15]. The application of a shear force on the system may lead to a break up of flocculated aggregates, and Hanai utilized this effect when he validated his formula up to a volume fraction of water equal to 0.8. [16].

Recently, in order to gain more information on the floc structures, we have adopted a concept suggested by Dukhin et al. [17]. The permittivity of the floc, ε_{f}, can be introduced as

$$\varepsilon^*_{\mathrm{f}} = f(\phi_{\mathrm{df}}, \varepsilon^*_1, \varepsilon^*_2) \,, \tag{4}$$

where ϕ_{df} is the volume fraction occupied by the droplets in the floc. Thus the total permittivity for the flocculated emulsion depends on the degree of flocculation

$$\varepsilon^*_{\mathrm{em}} = f(\phi_{\mathrm{f}}, \varepsilon^*_{\mathrm{f}}, \varepsilon^*_2) \tag{5}$$

with ϕ_{f} representing the volume fraction of flocs. In [5], we generalized this model by also taking into account the shape of the flocs and of the droplets in the flocs, i.e.,

$$\varepsilon^*_{\mathrm{f}} = f(\phi_{\mathrm{df}}, \varepsilon^*_1, \varepsilon^*_2, A_{\mathrm{df}}) \tag{6}$$

and

$$\varepsilon^*_{\mathrm{em}} = f(\phi_{\mathrm{f}}, \varepsilon^*_{\mathrm{f}}, \varepsilon^*_2, A_{\mathrm{f}}) , \qquad (7)$$

where A_{df} and A_{f} are the shape factors for the droplets in the flocs and for the floc, respectively.

The complex permittivity $\varepsilon^*_{\mathrm{f}}$ and the resulting $\varepsilon^*_{\mathrm{em}}$ are calculated by numerically solving, for instance, Eq. (3).

Rheology of emulsions

Very dilute emulsions will behave as simple liquid solutions and the viscosity is independent on the rate of shear (Newtonian flow behavior) [18]. The relative viscosity, η_{r}, for an emulsion containing a volume fraction ϕ disperse phase is then given by the Einstein equation [18–20];

$$\eta_{\mathrm{r}} = 1 + 2.5\phi , \qquad (8)$$

where $\eta_{\mathrm{r}} = \eta/\eta_0$. η and η_0 are the viscosities of the emulsion and the continuous phase respectively. It is assumed that no interaction between droplets take place and the increase in viscosity is a result of a modification of the flow pattern near the droplet surface. These assumptions holds only as long as $\phi < 0.01$–0.05 [20, 18].

In more concentrated emulsions the dependence between η_{r} and ϕ is more complex, and also other factors influence the flow properties of the system [18, 20–21]. The viscosities of the disperse phase and of the interfacial film [21], the droplet size, droplet size distribution, the droplet deformability and the interaction between the droplets all play important roles in this context. Thus, to describe the relation between ϕ and the viscosity, only semi-empirical models are available [20].

A Newtonian flow behavior cannot be expected for the more concentrated emulsions, and both plastic (i.e., a minimum shearing stress is required for flow to take place) and pseudoplastic (the flow takes place as soon as stress is applied) flows are often found for emulsified systems. These types of flow behavior have in common a progressive decrease of the viscosity as the shear stress is increased. However, above a limiting stress value the viscosity will in most cases remain unchanged. The plasticity (or pseudoplasticity) is due to, amount other factors, the flocculation of the emulsion droplets. The initial decrease in the viscosity as the shear stress is increased is a result of a partial disintegration of the floc structures. The stress-independent viscosity is reached when all the aggregates are broken down.

There seems to be an agreement that the flocculation/de-flocculation process governs the flow properties at low shear rates. However, the multitude of different floc shapes, floc densities, etc. that exist in emulsions makes it almost impossible to find a complete theoretical explanation on the non-Newtonian flow [18].

Experimental

Preparation of emulsions

The W/O emulsions were prepared by mixing dodecane and a NaCl-solution, with the volume fraction aqueous phase ranging from 0.50 to 0.95. The aqueous phase contained 4% NaCl by weight. The bulk conductivity at room temperature of this phase was 43.3 mS/cm, as measured by a CDM 83 Conductivity Meter (Radiometer, Copenhagen), operating at 50 kHz. As emulsifier Triton N-42 (Nonylphenoxypolyethoxyethanol) was used. The amount of surfactant was adjusted to 1% of the total volume of the emulsions.

After titrating the aqueous phase to the oil phase (with added surfactant) the mixture was vigorously shaken for 2 min by use of a vortex mixer (Vortex Genie 2, Scientific Industries). The emulsions were thereafter transferred to a viscometer of the coaxial cylinder type.

Rheology measurements

A coaxial type viscometer (Bohlin Visc 88 BV) was used. The outer cylinder had a inner diameter of 33.0 mm, whereas the diameter of the inner cylinder (measuring spindle) was 30 mm. The measuring spindle was made in a low-permittivity plastic material. The outer cylinder was made in brass.

The rotational speed of the spindle could be varied in eight steps from 20 rpm to 1000 rpm, corresponding to shear rates from 24 s^{-1} to 1230 s^{-1}. The viscosity was calculated after measuring the torque on the inner cylinder and its rotational speed [18].

Dielectric measurements

The dielectric spectra were measured by using the time domain dielectric spectroscopy (TDS) technique. The method of total reflection was used [22, 23], where the sample is placed at the end of a coaxial line. Through a threaded hole in the outer, stationary cylinder of the viscometer a flat dielectric cell was inserted (Fig. 1). This allowed us to make dielectric measurements on the emulsions both at rest and when a shearing force was applied (i.e., when the inner cylinder was rotated). The reflected pulses were observed in a time window of 40 ns. The pulses reflected from the empty cylinder and cylinder filled with

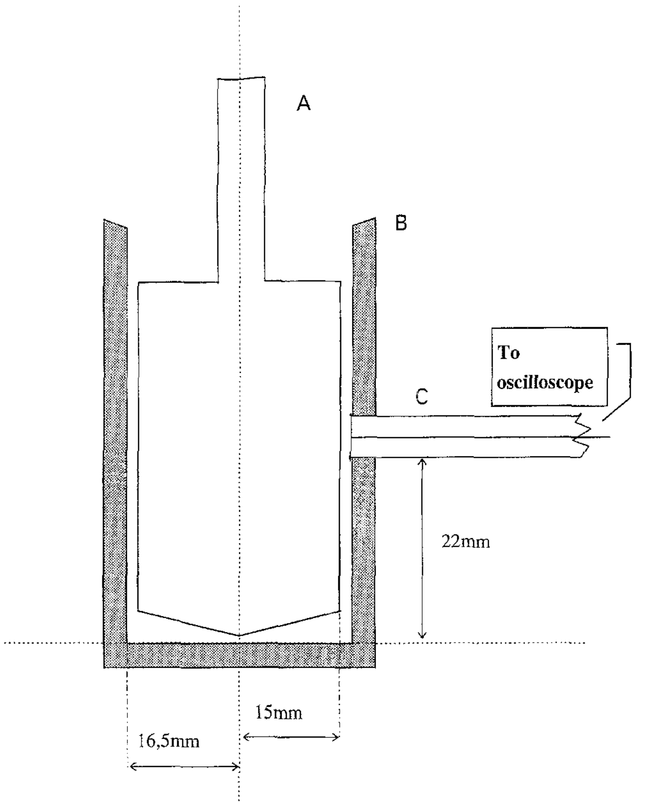

Fig. 1 Schematic view of the coaxial viscometer with the dielectric sensor inserted. **A** The inner cylinder (measuring spindle), **B** outer, stationary cylinder and **C** dielectric sensor

emulsion were Fourier transformed at 150 frequencies in the range from 25 MHz to 2 GHz, and the complex permittivity of the emulsion was calculated. Air was used as the reference substance. The cell length was found after calibration with six reference liquids with known permittivities, and determined to be 0.65 mm.

A Debye function,

$$\varepsilon^*(\omega) = \frac{\varepsilon_s - \varepsilon_\infty}{1 + i\omega\tau} + \varepsilon_\infty \tag{9}$$

was fitted to the experimental points. Here, ε_s is the static permittivity, ε_∞ the permittivity at high frequencies, τ is the relaxation time, and finally ω is the angular frequency. We have not included the relaxation of the aqueous phase in the fitting, as this gave only minor or no changes in the estimated parameters.

Experimental procedure

After transferring the emulsion into the outer cylinder of the viscometer dielectric measurements on the emulsion at rest were performed. At least 10 dielectric spectra were recorded, with 1-min intervals. The cylinder was mounted on the viscometer, on which the inner cylinder was already fixed. The dielectric measurements continued for several minutes at rest until the viscometer was started at the lowest rotational speed. Now the dielectric spectra were recorded at 30–60 s intervals over a period of 5–10 min. This was repeated for increasingly higher speeds up to the maximum speed attainable. After reaching the maximum speed we reduced it again while still recording rheological and dielectric data, until the shear rate was 0. At rest after finishing this cycle, dielectric spectra were recorded during various periods of time, ranging from 20 min to several hours.

For some of the samples we recorded spectra over a longer period at a given speed, while for other samples the speed settings were varied in a more random way.

Results and discussion

The mixing procedure applied cannot be expected to produce the smallest droplets, nor an extremely narrow droplet size distribution. This, and the relatively narrow range of shear for the viscometer limits the base set of the rheological data. We will therefore only discuss the main trends in these measurements.

In Figs. 2, 4 and 5, we have plotted the average values of the viscosity η, static permittivity ε_s and the dielectric relaxation times τ, respectively, versus the shear rate $\dot{\gamma}$. For the samples where it is of importance, the direction of the change in $\dot{\gamma}$ is indicated by the arrows (increasing rate: arrow to the right; decreasing rate: arrow to the left).

In Fig. 2 the average viscosity of the emulsions is plotted versus the shear rate. Figure 2A shows the results for the emulsions containing from 50 to 80% aqueous phase. The viscosity increases as the volume fraction disperse phase increases, due to a more pronounced hydrodynamic interaction between the droplets [20]. The shear thinning behavior (i.e., the viscosity becomes lower as higher shear rates are applied) can be ascribed to a progressive breakdown of flocculated structures [24].

For the emulsions with water contents of 80% and less, the rheology seemed to be relatively unaffected by the flow history. On the contrary, for the emulsions containing 85, 90 and 95% water, we note that the viscosity curves recorded for increasing shear rates do not coincide with the curves obtained when the rate is decreased. The viscosity is also higher after the maximal rate has been applied (Fig. 2B). The viscosity of concentrated emulsions is inversely proportional to the droplet diameter [20]. At the highest shear rate the energy input is sufficiently high to break down the largest droplets. Also the packing

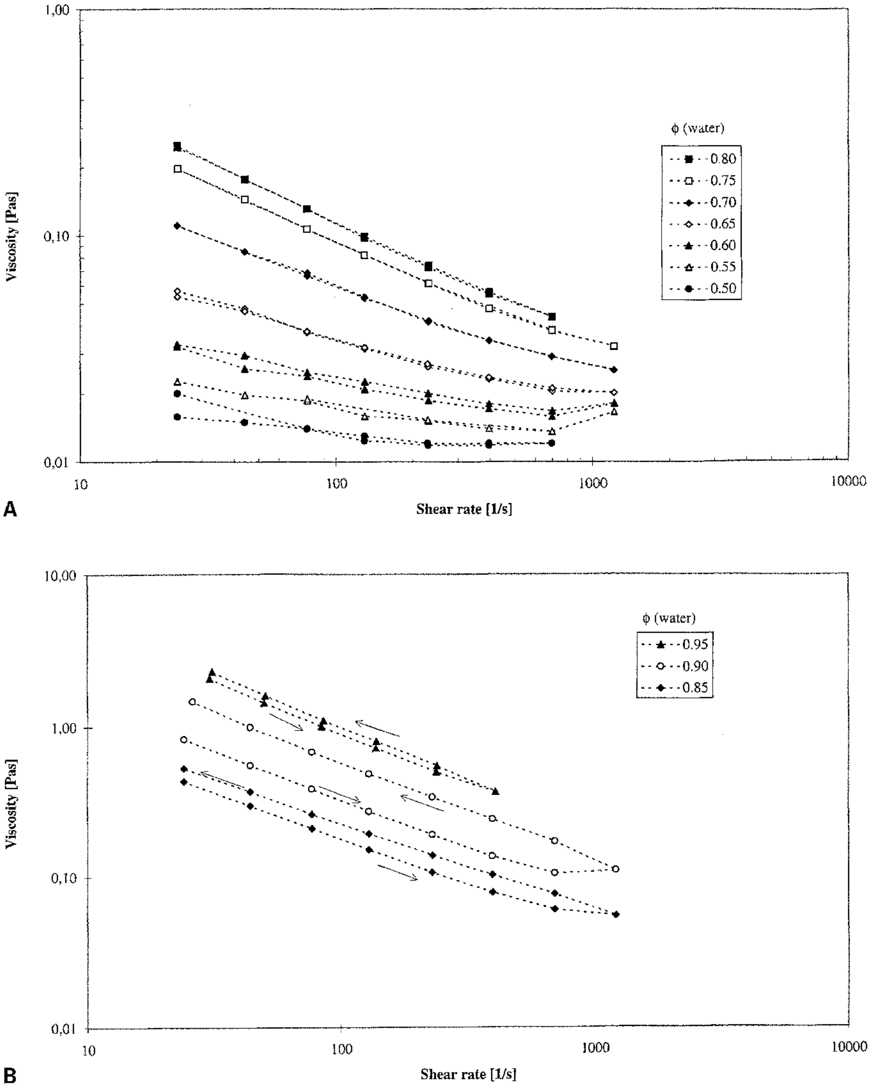

Fig. 2 The viscosity of w/o emulsions vs. shear rate. **A** Emulsions with volume fractions water ranging from 0.50 to 0.80. **B** Emulsions with volume fractions water ranging from 0.85 to 0.95

conditions will be altered when the emulsions are subjected to shear forces, and there will be a time dependence on the rearrangement of the droplets. The pronounced hysteresis observed is thus probably a result of a combination of these effects.

Also, the dielectric parameters show a very strong dependence on the shear rate. This is illustrated in Figs. 3 to 5. As an example, the dielectric spectra at various shear rates for an emulsion containing 80% water is given in Fig. 3A. Notable here are the changes in both the low frequency permittivity and the shift in the relaxation frequency. The high frequency permittivity is affected only to a small degree of variations in the shear rate. In Fig. 3B the variations in ε_s for the same emulsion during the complete measuring period are shown. It is noteworthy that the change in permittivity levels takes place instantaneously when the shear rate is altered. At constant shear rate the deviations in ε_s are small. The fall in permittivity after approximately 15 min occurred when the measuring spindle was forced into the outer cylinder. This action probably perturbed the state of the emulsion. However, when the emulsion was brought to rest again after measuring cycle, the initial permittivity level was almost reached.

Figure 4A shows the average static permittivity for the emulsions with water contents up to 80%. (Please note that the permittivities marked on the Y-axis are measured when the emulsions are at rest, i.e., no shear force is applied.) Application of a shear force leads to a drastic reduction in ε_s. The largest decrease, both in absolute value and relative to the permittivity at the highest shear rate is found for the emulsions containing 80 and 85% water (Fig. 4B). For these two samples the static permittivity is reduced from 324 to 60 and from 630 to 90, respectively. Except for the 70% and 80% emulsions, ε_s is unaffected by

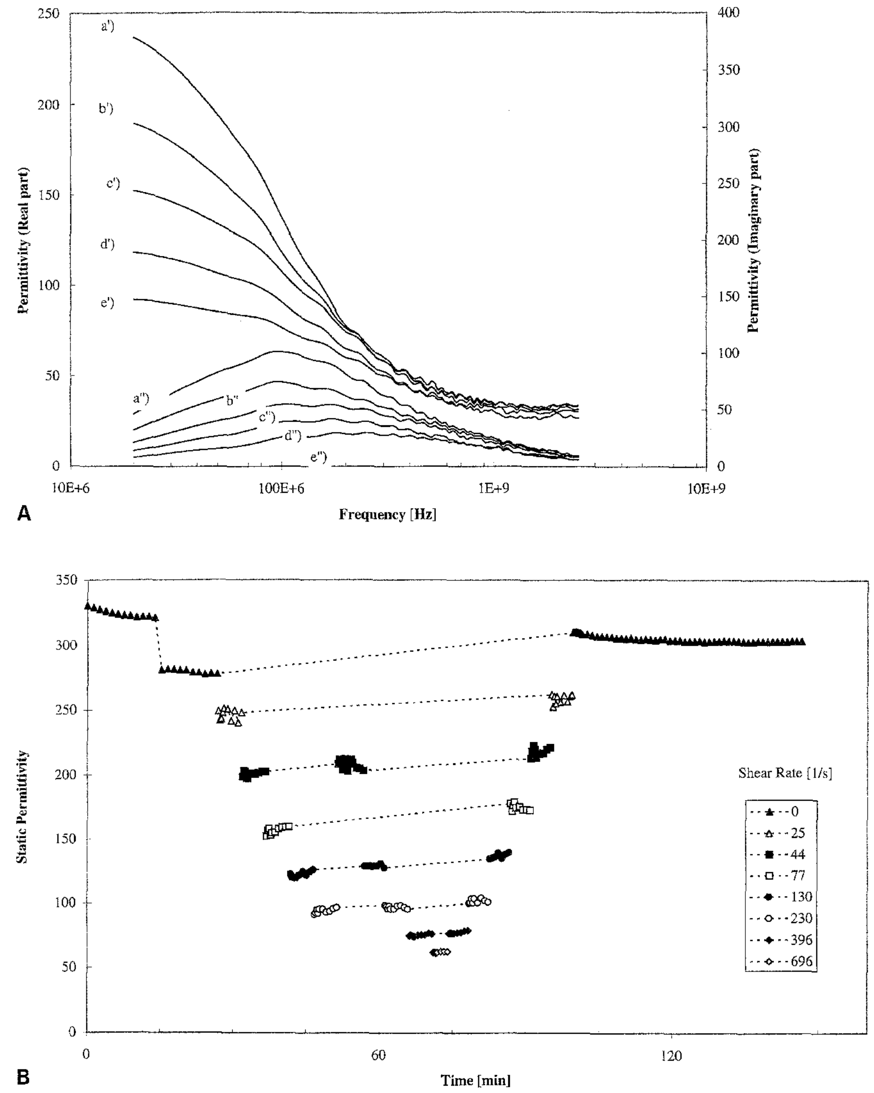

Fig. 3 **A** The dielectric spectra of an emulsion with 80% water at various shear rates. The real parts are denoted (′) while the imaginary parts of the spectra are denoted (″). The shear rates are 25 s^{-1} (*a*′, *a*″), 44 s^{-1} (*b*′, *b*″), 77 s^{-1} (*c*′, *c*″) 130 s^{-1} (*d*′, *d*″) and 230 s^{-1} (*e*′, *e*″), respectively. **B** The static permittivity as a function of time during a complete measuring cycle. Measurements performed at the same shear rate are marked with similar symbols

the flow history, i.e., for a given volume fraction disperse phase and a given shear rate the permittivity is fairly constant. For emulsions with 85, 90 and 95% aqueous phase the static permittivity at rest is very high (Fig. 4B). Again, a reduction in ε_s when the shear rate increases is observed. However, when the shear rate is reduced from the maximum towards lower rates, ε_s does not take on the same values as recorded when $\dot{\gamma}$ increased. At the highest rates, ε_s attains higher values (for 85 and 90% emulsions), while at low $\dot{\gamma}$ the static permittivity reaches only substantially lower levels. Thus the hysteresis effect observed in the rheology data is reflected in anomalies in the dielectric data.

The relaxation times show the same trend as the static permittivity (Fig. 5A, B). At rest or at low shear rates τ is high, and an increase in $\dot{\gamma}$ results in a marked reduction in τ. The hysteresis effect in the most concentrated emulsions is reflected also in this parameter. At low rates of shear one finds that the relaxation time increases as the volume fraction water increases. This is expected from, for instance, Eq. (1), given that the bulk conductivity of the disperse phase is equal for all the samples. However, the shear rate dependence of the relaxation time is not very pronounced for the least concentrated emulsions (50% and 55%) thus at intermediate and high shear rates the relaxation in these emulsions is actually slower than in the more concentrated ones (Fig. 5A).

The averaged values of the static permittivity and the relaxation times at the various shear rates are plotted versus the volume fraction disperse phase in Figs. 6 and 7, respectively. In the same plots we also show the theoretically predicted parameters for a system consisting of independent droplets, as calculated by use of Eq. (1). For the samples containing 80% water or less, we note that the

Fig. 4 The static permittivity of w/o emulsions vs. shear rate. **A** Emulsions with volume fractions water ranging from 0.50 to 0.80. **B** Emulsions with volume fractions water ranging from 0.85 to 0.95

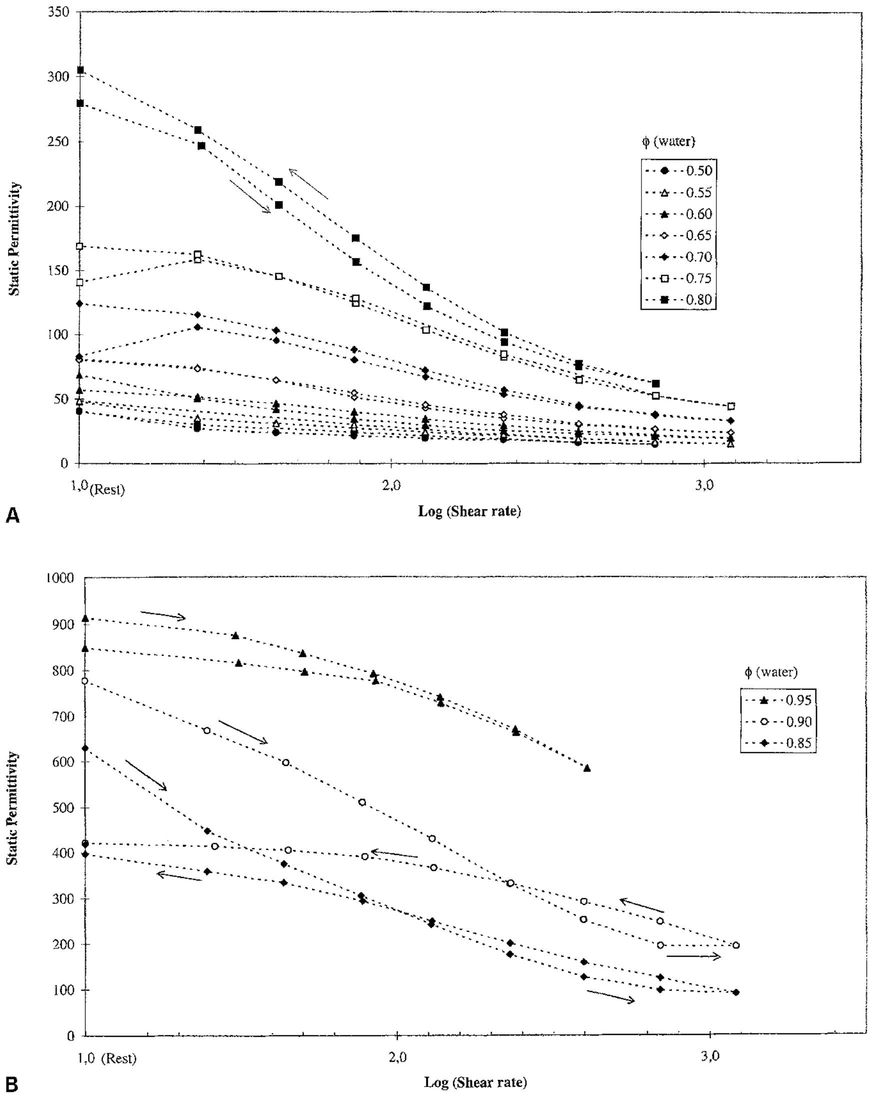

static permittivity at rest or at low shear rates is higher than predicted from Eq. (1), but when the shear rate is increased the experimental values approach the theoretical ones. This effect was also observed by Hanai [9], and is probably due to the de-flocculation of the emulsions. However, the static permittivity continues to decrease to levels far below the Hanai-curve as the shear rate is further increased. Also, the relaxation times show the same trends as ε_s when the rate of shear changes (Fig. 7). This behavior can be explained if one assumes that the emulsion droplets at these shear rates become increasingly elongated, and oriented in the direction of the flow in the viscometer. If this is the case, Eq. (2) can be applied and, in principle, the axial ratio of the droplets can be found (from A_i). Unfortunately, it is difficult to find one single A_i that at the same time explains the static permittivity *and* the relaxation time for a given sample at a given shear rate. When comparing Figs. 6 and 7, we note that the rate of shear for which ε_s is closest to the values from Eq. (1) is in general lower than the corresponding rate for the relaxation times.

For the emulsions of the highest internal phase concentrations (i.e., $\phi \geq 0.85$), both ε_s and τ lay below the Hanai-curve in all the measurements, also when no shear is applied. At these high concentrations the droplets cannot take on a spherical shape, and an irregular polyhedric shape is more probable [25]. Thus Eq. (1) should not be expected to give reliable estimates of the dielectric parameters for these samples.

Conclusions

One common determining factor in the theoretical treatment of the rheological and dielectric properties of

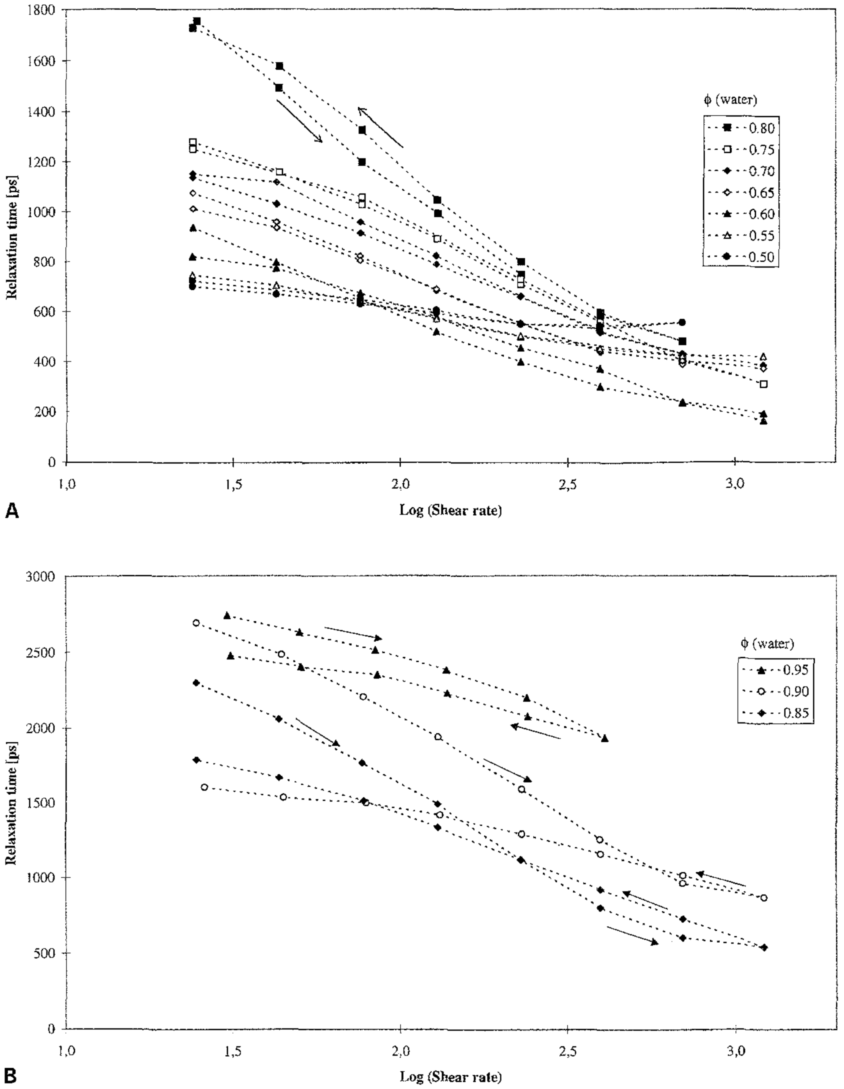

Fig. 5 The relaxation time of w/o emulsions vs. shear rate. **A** Emulsions with volume fractions water ranging from 0.50 to 0.80. **B** Emulsions with volume fractions water ranging from 0.85 to 0.95

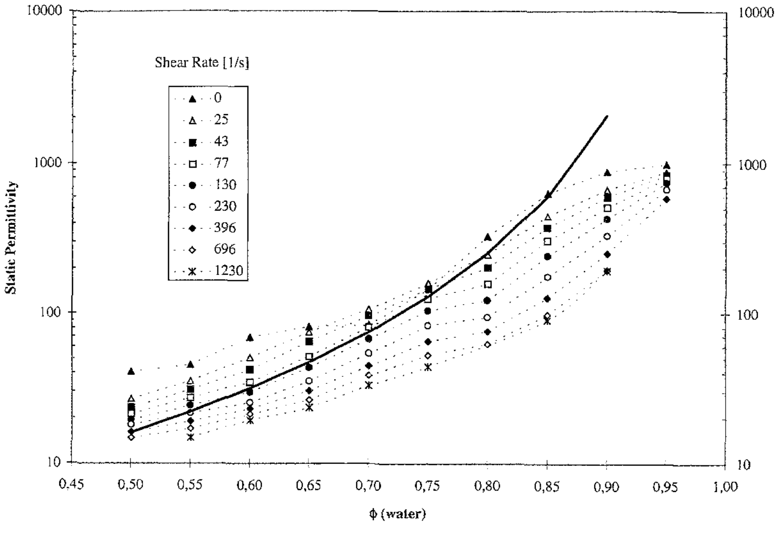

Fig. 6 The static permittivity of w/o emulsions vs. volume fraction water. The bold line corresponds to values calculated from Eq. (1)

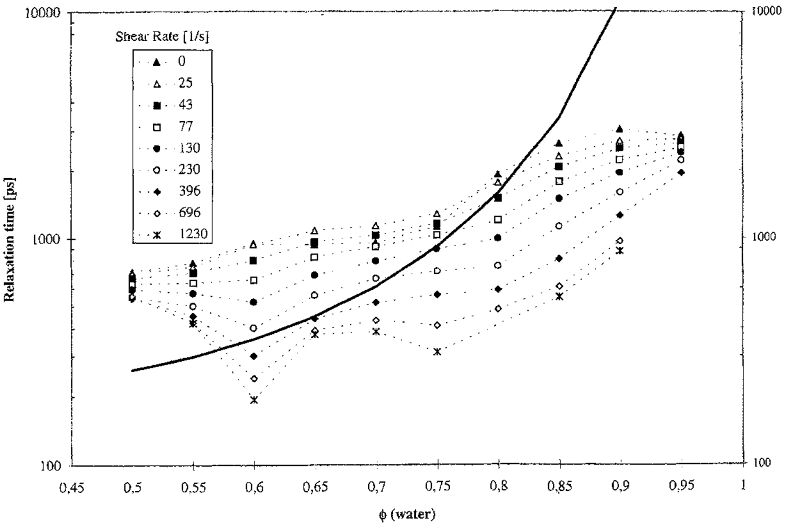

Fig. 7 The relaxation times of w/o emulsions vs. volume fraction water. The bold line corresponds to values calculated from Eq. (1)

emulsions is the degree of flocculation. With the device presented in this work we have shown that there is a connection between the viscosity and the dielectric properties of w/o emulsions subjected to shear forces. It would be of interest to extend the range towards both lower and higher shear rates in order to cover the de-flocculation process in more detail. By improving the experimental set-up and combining the rheological and dielectric data, one may be able to extract valuable information on the flocculation in the emulsified systems.

Acknowledgments Tore Skodvin would like to acknowledge the STP program "Surface and Colloid Chemistry for the Oil Industry", financed by the Norwegian Research Council (NFR) and the oil companies Elf Aquitaine, Saga Petroleum A/S and Statoil A/S for a Ph.D. grant. The dielectric instrumentation was also financed by NFR.

References

1. Sjöblom J, Førdedal H, Skodvin T (1996) In: Sjöblom J (ed) Emulsions and Emulsion Stability. Surfactant Science Series, Marcel Dekker, New York
2. Gestblom B, Førdedal H, Sjöblom J (1994) J Dispersion Sci Technol 15:449
3. Førdedal H, Nodland E, Sjöblom J, Kvalheim OM (1995) J Colloid Interface Sci 173:396
4. Skodvin T, Sjöblom J, Urdahl O, Gestblom B (1994) J Colloid Interface Sci 166:43
5. Sjöblom J, Skodvin T, Jakobsen T, Dukhin SS (1994) J Dispersion Sci Technol 15:401
6. Skodvin T, Jakobsen T, Sjöblom J (1994) J Dispersion Sci Technol 15:423
7. Skodvin T, Sjöblom J, Saeten JO, Wärnheinm T, Gestblom B (1994) Colloids Surfaces A 83:75
8. Hanai T (1960) Kolloid Z 171:23
9. Hanai T (1961) Kolloid Z 175:61
10. Boned C, Peyrelasse J (1983) J Colloid Polym Sci 261:600
11. Boyle MH (1985) Colloid Polym Sci 263:51
12. Wagner KW (1914) Arch Electrotechn 2:371
13. Wiener O (1912) Abh Sächs Akad Wiss 32:509
14. Bruggeman DAG (1935) Ann Phys Lpz 24:636
15. Parts AG (1945) Nature 155:236
16. Hanai T (1961) Kolloid Z 177:57
17. Dukhin SS, Shilov VN (1974) Dielectric Phenomena and the Double Layer in Disperse Systems and Polyelectrolytes, Wiley, New York, pp 136
18. Sherman P (1969) In: Sherman P (ed) Emulsions Science, Ch 4. Academic Press, London, 1969
19. Einstein A (1906) Investigations on the Theory of the Brownian Movement. Dover, New York
20. Thadros ThF (1994) Colloids Surfaces A: Physicochem Eng Aspects 91:39
21. Thadros ThF (1992) In: Sjöblom J (ed) Emulsions - A Fundamental and Practical Approach. NATO ASI Series, Series C - Vol 363, Kluwer Academic Publishers, Dordrecht, p 173
22. Cole RH, Mashimo S, Winsor IV P (1980) J Phys Chem 84:786
23. Cole RH, Berberian JG, Nashimo S, Chryssikos G, Burns A, Tombari E (1989) J Appl Phys 66:793
24. Pal R (1993) Colloids Surfaces A: Physicochem Eng Aspects 71:173
25. Davies HT (1994) Colloids Surfaces A: Physicochemical Eng Aspects 91:9